Journal of Vibration and Acoustics, Vol. 120, Oct. 1998, pp. 949-957

EXPERIMENTAL DETERMINATION OF LOCAL STRUCTURAL STIFFNESS BY DISASSEMBLY OF MEASURED FLEXIBILITY MATRICES

Scott W. Doebling[1]

Engineering Sciences and Applications Division
Engineering Analysis Group (ESA-EA)
Los Alamos National Laboratory
M/S P946, Los Alamos, NM, 87545

Lee D. Peterson[2]

Center for Aerospace Structures and
Department of Aerospace Engineering Sciences
University of Colorado, Boulder, Colorado 80309-0429

Kenneth F. Alvin[3]

Structural Dynamics and Vibration Control Dept.
Sandia National Laboratories
M/S 0439, Albuquerque, NM, 87185-5800

ABSTRACT

A new method is presented for identifying the local stiffness of a structure from vibration test data. The method is based on a projection of the experimentally measured flexibility matrix onto the strain energy distribution in local elements or regional superelements. Using both a presumed connectivity and a presumed strain energy distribution pattern, the method forms a well-determined linear least squares problem for elemental stiffness matrix eigenvalues. These eigenvalues are directly proportional to the stiffnesses of individual elements or superelements, including the cross-sectional bending stiffnesses of beams, plates, and shells, for example. An important part of the methodology is the formulation of nodal degrees of freedom as functions of the measured sensor degrees of freedom to account for the location offsets which are present in physical sensor measurements. Numerical and experimental results are presented which show the application of the approach to

1. Technical Staff Member, Associate Member ASME, doebling@lanl.gov, (505) 667-6950
2. Associate Professor, Senior Member ASME, Lee.Peterson@Colorado.EDU, (303) 492-1743
3. Senior Member of Technical Staff, kfalvin@sandia.gov, (505) 844-9329

example problems.

NOMENCLATURE

$[A]$	Stiffness connectivity matrix
d	Node-to-sensor offset distance
EI	Beam cross-sectional bending stiffness parameter
$\{f\}$	Applied force vector
GJ	Beam cross-sectional torsional stiffness parameter
$[G]$	Structural flexibility matrix
$[I]_a$	Identity matrix of size $(a \times a)$
$[K]$	Structural stiffness matrix
$[L]$, $[H]$	Transformations between sensor and global degrees of freedom
L	Length of structural finite element
$[M]$	Structural mass matrix
n_e	Number of finite elements or superelements in model
n_g	Number of global degrees of freedom in model
n_m	Number of measurement sensor degrees of freedom
n_p	Number of stiffness eigenvalues for entire structure or superelement
n_α	Number of elemental degrees of freedom in α^{th} finite element
$[p]$	Diagonal matrix of elemental stiffness eigenvalues
$[P]$	Diagonal matrix of assembled stiffness eigenvalues for entire structure or superelement

r_α	Rank of α^{th} elemental stiffness matrix
$[T]$	Transformation matrix from global to elemental coordinates
$\{u\}$	Displacement vector
U, U_c	Strain energy and complimentary strain energy
$[\Phi]$	Matrix of dynamic structural eigenvectors (mode shapes)
$[\kappa]$	Static eigenvector matrix
$[\Lambda]$	Diagonal matrix of dynamic structural eigenvalues (modal frequencies squared)

Superscripts

G	Global degree of freedom set
E	Elemental degree of freedom set
M	Measured degree of freedom set

Subscripts

A	Analytical prediction
n	Measured modal properties
r	Residual modal properties
α	Index indicating element number (property of α^{th} finite element)

INTRODUCTION

An important facet of state-of-the-art structural technology is the ability to determine and monitor the mechanical condition of an aerospace, civil, automotive, or other structure during both manufacture and operation. Such a capability would lower fabrication costs and ensure that both performance and safety are maintained during the structural lifetime. Such technology enables the measurement and identification of the localized stiffness of

manufactured components, as well as the detection of errors, flaws, and damage resulting from fabrication. This technology also enables the development of high fidelity finite element models (FEMs) early in the design cycle by allowing validation of local structural stiffness values at the junctions and interfaces within prototype structural hardware.

The diagnosis of the mechanical condition of a structure is primarily a problem of determining the mass and stiffness distribution within the structure, using a few discrete measurements of the vibration response. This issue remains largely unsolved primarily because it is an inverse modeling problem. Ordinarily, structural analysis begins with an assumed set of mechanical properties, from which the dynamic response is simulated. In the current problem, however, the known quantity is the dynamic response, from which the mechanical properties must be extracted. A significant amount of research in this area has focused on the use of a detailed dynamic finite element model to determine the local mechanical properties. In these methods, the error between modal test data and predicted finite element modal behavior is minimized by adjusting the parameters which determine the finite element model stiffness and mass distribution. While these methods are generally successful at updating the dynamic model, they ordinarily involve the computationally intensive minimization of a nonlinear error norm, and, consequently, are not necessarily appropriate for on-line, real-time data analysis and damage diagnostics.

A set of algorithms more suitable for on-line monitoring can be found in Kaouk and Zimmerman (1994), Lim and Kashangaki (1994), and Sheinman (1994). In these methods, the deviation of the stiffness and mass from a preexisting finite element model is indicated by residual modal force errors at nodes in the model. These methods indicate the degrees of freedom (DOF) associated with error or damage, and, using appropriate elemental pro-

jections, can determine the magnitude of stiffness errors within the structure. However, these techniques rely exclusively on a subset of measured modal parameters, i.e. the methods require the analyst to select which of the measured vibration mode shapes and modal frequencies will be used in the algorithm. This shortcoming is one factor that discourages the use of these otherwise attractive methods. Because the modes themselves may change significantly when the stiffness changes, the comparison may be significantly biased by the selection of modes to include in the comparison set. There is little physical intuition available for the selection of these modes. Also, these methods find the magnitude of *nodally concentrated* errors and stiffness changes, so it is difficult to use them to localize the elemental stiffness errors and changes when the structure has load-path redundancy. A procedure to localize structural damage using a residual modal force error by computing perturbations to the elemental stiffness parameters was presented by Doebling (1996). This technique overcame the limitations of some of the previously mentioned methods based on global nodal stiffness quantities, but did not overcome the limitations associated with mode selection, i.e. it was still necessary to select a subset of the measured modal parameters to use in the computations.

The approach that has been the most successful at eliminating the need for selecting a subset of the measured modal parameters uses the mode information in the form of the structural flexibility matrix. The structural flexibility matrix is defined (for a structure with no rigid body modes) as the inverse of the static stiffness matrix. Thus, for a generalized static displacement vector in global FEM coordinates, $\{u^G\}$, and a generalized static force vector in global FEM coordinates, $\{f^G\}$, the stiffness and flexibility matrices can be defined as

$$\{f^G\} = [K^G]\{u^G\} \qquad \{u^G\} = [G^G]\{f^G\} \tag{1}$$

If the full set of structural mode shapes in the global FEM coordinate set, $[\Phi^G]$, is known, then the static flexibility matrix can be formed via

$$[K^G]^{-1} = [G^G] = [\Phi^G][\Lambda]^{-1}[\Phi^G]^T \tag{2}$$

where $[\Lambda]$ is a diagonal matrix of the modal frequencies squared. In practice, however, a subset of the total number of structural modes is actually measured. Denoting the measured mode shapes in the global DOF set as $[\Phi_n^G]$ and the diagonal matrix of measured model frequencies squared as $[\Lambda_n]$, then the structural flexibility matrix in the global FEM DOF set $[G^G]$, can be formed via

$$[G^G] = [\Phi_n^G][\Lambda_n]^{-1}[\Phi_n^G]^T + [G_r^G] \tag{3}$$

where $[G_r^G]$ is the "residual flexibility matrix" representing the contributions to $[G^G]$ from the unmeasured modes. Likewise, the structural flexibility matrix in the experimental measurement DOF set $[G^M]$, can be formed using the measured mode shapes in the experimental measurement DOF set $[\Phi_n^M]$ as

$$[G^M] = [\Phi_n^M][\Lambda_n]^{-1}[\Phi_n^M]^T + [G_r^M] \tag{4}$$

Efficient, reliable methods for measuring perhaps 60 to 100 modes of a structure have made it possible to determine accurate structural flexibility matrices using Eq. (4), although the success is largely dependent on the quality of the experimental configuration and the system identification algorithm used in the data analysis (see Peterson, 1995, Peterson and Alvin, 1997). One limitation on the accuracy of flexibility estimation is the inability to determine the full residual flexibility matrix under practical testing constraints. This issue is discussed by Doebling, et al. (1996), where a method is presented for estimating the full residual flexibility matrix when the excitations and responses are not fully collocated.

Some techniques that have been used to analyze the measured flexibility matrix to determine local stiffness changes in the structure involve estimating the rank-deficient global structural stiffness matrix in measurement coordinates, $[K_n^M]$, from the measured flexibility matrix using a pseudoinverse operator (see Strang, 1988). The basic equation for these techniques is:

$$[K_n^M] = [G_n^M]^+ = ([\Phi_n^M][\Lambda_n]^{-1}[\Phi_n^M]^T)^+ \tag{5}$$

The pseudoinverse is used in this case rather than the strict inverse because the modal flexibility matrix $[G_n^M]$, which is formed only from the measured mode shapes and modal frequencies (not including the effects of residual flexibility), is rank deficient when the number of measured modes is less than the number of measurement sensors. The formulation of the "measured" stiffness matrix in this manner was proposed by Alvin, et al. (1995) and was employed by Peterson, et al. (1993) for the purpose of damage identification by comparing the measured stiffness matrices before and after damage had occurred. Although this technique circumvented the problems associated with selection of modes by simply using all of the identified modes in Eq. (5), the method had no way of preserving the proper load paths in the structure. Thus for a redundant (statically indeterminate) structure, the elemental stiffness parameters could not be extracted. Also, the pseudoinversion of the measured flexibility spreads the error, which tends to be concentrated in specific partitions of $[G_n^M]$, throughout all the stiffness matrix entries, so that it is difficult to isolate the specific elements which have a high error content.

This paper presents a generalized method for the determination of local stiffness parameters based on the decomposition of the measured flexibility matrix into the individual stiffness parameters of an assumed set of superelements within the structure. The presumption

is that the load paths of the structure are known within superelements whose boundaries are defined by the measurement sensors. Using the presumed connectivity and strain energy distribution pattern, a solution of the "flexibility matrix disassembly problem" is presented which always determines a unique solution for the stiffness parameters of the superelements. The use of the flexibility matrix rather than individual modes circumvents the problems with mode selection. The use of the flexibility matrix rather than the measured stiffness matrix circumvents the problems associated with the pseudoinversion of the flexibility matrix. Additionally, the use of an assumed set of elemental connectivity ensures that the computed elemental stiffness values will be consistent with the load paths in the structure as idealized by a finite element model.

The key to this procedure is the fact that any structural superelement can be presumed to be a combination of elemental stiffness eigenvectors, which correspond to statically equilibrated static deformation shapes of the structure. (These should not be confused with the structural $[M]$ and $[K]$ eigenvectors, which are associated with modes of vibration). A well-determined linear problem is defined, which can be solved for the elemental stiffness eigenvalues of the presumed superelements. These elemental stiffness eigenvalues correspond to elemental stiffness parameters such as *EA*, *EI*, and *GJ*. For example, for 2DOF truss elements, the stiffness parameters are the longitudinal spring stiffnesses; for beams in three dimensions they are the extensional stiffness, the torsional stiffness, and the two cross-sectional bending stiffnesses; and for plates they are the corresponding bending and extensional stiffnesses. More general elements, including those for orthotropic materials and shells, are also included within this framework. However, these elements require the addition of linear side constraints on the stiffness parameters. It should be noted that

any superelement can be included provided there is an underlying set of shape functions or other parameters which define the elemental strain energy distribution.

The practical implementation of the flexibility disassembly method requires the consideration of how measurement degrees of freedom at the sensors correspond to the nodal degrees of freedom used in the corresponding superelement discretization. This consideration compensates for the fact that the global DOF measurements are generally inferred from translational sensor measurements made at several locations which are physically offset from the node. The measurement sensors are presumed to fully determine or overdetermine the nodal degrees of freedom at a point by rigid connections. This requirement results in a well-formulated linear algebra problem to solve for the flexibility matrix in FEM DOF from measurement DOF.

The paper is organized as follows: The first section presents the theory whereby the global stiffness matrix is parameterized using the elemental stiffness eigenvalues and eigenvectors. The second section formulates the disassembly problem to solve for the elemental stiffness eigenvalues using a known global stiffness matrix and elemental stiffness eigenvectors. Next, the theory for applying disassembly to the global flexibility matrix is presented, where an equivalence of complementary and ordinary strain energy is used to formulate a square, invertible linear algebra problem for the local stiffness parameters. The projection of the nodal DOF onto the measurement DOF is considered next, allowing the flexibility disassembly process to be applied to an experimentally measured flexibility matrix. The paper concludes with application of the technique to numerical and experimental data from a cantilevered beam.

PARAMETERIZATION OF THE ELEMENTAL AND GLOBAL STIFFNESS MATRICES

This section presents the formulation of the quantities necessary for the disassembly of the measured stiffness and flexibility matrices. Begin by presuming that the global stiffness of the structure can be modeled using an assemblage of n_e finite elements or superelements, connecting n_g global DOF, $\{u^G\}$. Each of the n_e elements itself connects elemental DOF for the α^{th} element, $\{u^E\}_\alpha$, which has size $(n_\alpha \times 1)$. The corresponding $(n_\alpha \times n_\alpha)$ elemental stiffness matrix in this coordinate basis is $[K^E]_\alpha$. If the elemental DOF are related by a rectangular transformation $[T]_\alpha$ to the global DOF as

$$\{u^E\}_\alpha = [T]_\alpha \{u^G\} \tag{6}$$

then the global stiffness matrix can be formed by assembling all the elemental matrices according to

$$[K^G] = \sum_{\alpha = 1}^{n_e} [T]_\alpha^T [K^E]_\alpha [T]_\alpha \tag{7}$$

The $(n_\alpha \times n_g)$ elemental-to-global DOF transformation matrices $[T]_\alpha$ include coordinate rotations from the elemental frames to the global frame, the table lookup for the correspondence between elemental and global DOF, and the effect of constraints such as pinned or fixed connections.

It is important to note that Eq. (7) is not a minimum-rank definition of the disassembly problem, because only some of the unknowns in the elemental matrices $[K^E]_\alpha$ are independent. Thus, besides being symmetric, each elemental stiffness matrix is always rank-deficient. Because $[K^E]_\alpha$ is symmetric, it has $(n_\alpha(n_\alpha + 1))/2$ unknown entries, but because of its rank, only a few of these are actually independent unknowns. Consider as an example

a simple spring element connecting two nodes, each of which includes three *(x,y,z)* displacements as DOF. Because this elemental stiffness matrix is 6x6, it potentially has 21 unknown elements. However, the rank of the elemental stiffness matrix is only 1 because of the stiffness connectivity, and therefore the stiffness of the element is completely specified by the value of 1 unknown parameter, which, in this case, is the axial stiffness of the spring.

In general, then, it is necessary to decompose the rank r_α elemental stiffness matrix $[K^E]_\alpha$ into its static eigenvalues and eigenvectors so that

$$[K^E]_\alpha = [\kappa]_\alpha [p]_\alpha [\kappa]_\alpha^T \tag{8}$$

in which $[\kappa]_\alpha$ is the $n_\alpha \times r_\alpha$ matrix of static eigenvectors for the α^{th} element, and $[p]_\alpha$ is a diagonal matrix of size $(r_\alpha \times r_\alpha)$ containing the nonzero static eigenvalues $\{p\}_\alpha$ for the α^{th} element. Physically, the columns of $[\kappa]_\alpha$ are the distinct, statically equilibrated deformation shapes of the element which have nonzero strain energy. They are normalized to have unit magnitude, such that

$$[\kappa]_\alpha^T [\kappa]_\alpha = [I]_{r_\alpha} \tag{9}$$

The static decomposition of Eq. (8) can be substituted into Eq. (7) to get

$$[K^G] = \sum_{\alpha=1}^{n_e} [T]_\alpha^T [\kappa]_\alpha [p]_\alpha [\kappa]_\alpha^T [T]_\alpha \tag{10}$$

This expression can be further simplified to

$$[K^G] = [A][P][A]^T \tag{11}$$

where the "stiffness connectivity matrix" $[A]$ is a sparse matrix defined by

$$[A] = [([T]_1^T [\kappa]_1) \quad ([T]_2^T [\kappa]_2) \quad \dots \quad ([T]_{n_e}^T [\kappa]_{n_e})] \tag{12}$$

and $[P]$ is a diagonal matrix, size $(n_p \times n_p)$, of the assembled elemental stiffness eigenvalues $\{P\}$ where

$$\{P\} = \begin{Bmatrix} \{p\}_1 \\ \{p\}_2 \\ \cdots \\ \{p\}_{n_e} \end{Bmatrix} = \begin{Bmatrix} P_1 \\ P_2 \\ \cdots \\ P_{n_p} \end{Bmatrix} \qquad (13)$$

$$n_p = \sum_{\alpha = 1}^{n_e} r_\alpha$$

The columns of $[A]$ mathematically embody the connectivity of the structure by defining how a particular superelement stiffness parameter P_i influences the stiffness at the structural DOF. It is important to note that Eq. (11) does not imply that the $\{P\}$ are the eigenvalues of $[K^G]$. This is because the columns of $[A]$ do not generally form an orthogonal basis for the global stiffness matrix $[K^G]$.

Examples of Elemental Stiffness Parameterization for Representative Elements

Most generally, the columns of $[\kappa]_\alpha$ can be considered to be the eigenvectors of the static condensation of a superelement's stiffness matrix onto its boundary DOF. In this sense, they can be derived from a solution of a partial differential equation or a finite element model. The only constraint is that the resulting stiffness parameters $\{p\}_\alpha$ must have a physical interpretation in terms of the stiffness of the superelement. Consider as a first example a spring or truss element with stiffness k connecting two nodes, as shown in Figure 1. For this element, the stiffness matrix is

$$[K^E] = \begin{bmatrix} k & -k \\ -k & k \end{bmatrix} \qquad \{u^E\} = \begin{Bmatrix} u_1 \\ u_2 \end{Bmatrix} \qquad (14)$$

Computing the eigen-decomposition on $[K^E]$ yields the corresponding stiffness eigenvec-

tors and eigenvalues:

$$[\kappa] = \begin{bmatrix} \frac{1}{\sqrt{2}} \\ -\frac{1}{\sqrt{2}} \end{bmatrix} \qquad \{p\} = 2k \tag{15}$$

As a second example, consider a beam element connecting two 6 DOF nodes, as shown in Figure 1. For this element, the elemental DOF are

$$\{u^E\} = \left\lfloor u_1 v_1 w_1 \theta_{x_1} \theta_{y_1} \theta_{z_1} u_2 v_2 w_2 \theta_{x_2} \theta_{y_2} \theta_{z_2} \right\rfloor^T \tag{16}$$

and the corresponding stiffness eigenvectors and parameters are listed in Appendix A. Notice that for each beam cross-sectional bending stiffness, there are two corresponding parameters. In any calculation for the parameters, each pair of bending eigenvalues are constrained through their linear dependence on the corresponding EI.

It should be noted that the existence of the unusual mixed units of length and radians in the beam element eigenvectors is a consequence of the orthonormality of $[\kappa]$ and the units of the displacement vector of the beam element. The mixed units do not affect the units of the resulting stiffness matrix. The mixed units arise because the displacement vector for the beam element contains DOF of both length and angle units. By analogy, observe that the units of the 2-norm of a vector with mixed units will have mixed units. When the elemental stiffness matrix is formed using these mixed-unit eigenvectors and eigenvalues, the linear combinations of parameters cancel out the mixed units leaving each entry in the matrix with only a single unit definition. Thus, the mixed units merely exist in the intermediate quantities $[\kappa]$, $[A]$, and $[P]$, and not in the elemental or global stiffness matrices.

DISASSEMBLY OF THE GLOBAL STIFFNESS MATRIX IN GLOBAL COORDINATES

In this section, the disassembly procedure is outlined and applied to the global stiffness matrix, $[K^G]$. While the disassembly of the global stiffness matrix is not practical to implement on measured data, it is useful for illustrating the derivation of global flexibility matrix disassembly. Consider the situation where the global stiffness matrix $[K^G]$ and a connectivity matrix $[A]$ are known, and the stiffness parameters $\{P\}$ are to be determined. The corresponding problem statement contained in Eq. (11) includes as unknowns the n_p elements of $\{P\}$. The number of equations is equal to the number of unique elements in $[K^G]$. Because of symmetry, there are $(n_g(n_g+1))/2$ equations and n_p unknowns. Except for the pathological case in which the assumed connectivity has precisely redundant load paths in its element definitions, there can never be more unknowns than equations. An example of such a case is a pair of springs in parallel between the same DOF, such that two columns of $[A]$ are identical. Even for a completely redundant structure the solution is overdetermined, because in such a structure there is an equivalent spring from each DOF to each other DOF and from each DOF to ground for a total of $(n_g(n_g+1))/2$ unknown elements of $\{P\}$. Thus, it will be true that for any structure with a non-pathological presumed connectivity that

$$n_p \leq \frac{n_g(n_g+1)}{2} \tag{17}$$

Consequently, the above disassembly problem always has fewer unknowns than equations, and thus a unique least-squares solution always exists.

To compute the solution to this problem, however, it is necessary to recast the matrix formulation of Eq. (11) in a form amenable to linear equation solvers by writing down each

element. The most convenient form is summation (tensor) notation, in which repeated indices indicate a sum over the values of that index, as shown in Zienkiewicz and Taylor (1994). Define K_{ij}^G to be the tensor equivalent of $[K^G]$, define $A_{i\beta}$ to be the tensor equivalent of $[A]$, and define P_β to be the tensor equivalent of $\{P\}$. In this notation, $i, j \in \{1 \ldots n_g\}$ and $\beta \in \{1 \ldots n_p\}$. Then, Eq. (11) can be written as

$$\begin{aligned} K_{ij}^G &= A_{i\beta} P_\beta A_{j\beta} \\ &= (A_{i\beta} A_{j\beta}) P_\beta \end{aligned} \tag{18}$$

This tensor equation is equivalent to the following linear algebra problem

$$[C]\{P\} = \{B\} \tag{19}$$

in which $\{B\}$ is formed from the $(n_g(n_g + 1))/2$ unique elements of K_{ij}^G by cycling i from 1 to n_g and j from i to n_g. The corresponding (i, j) row of $[C]$ is given by

$$\lfloor C_{ij} \rfloor = \left\lfloor \; A_{i1}A_{j1} \; A_{i2}A_{j2} \; \ldots \; A_{in_p}A_{jn_p} \; \right\rfloor \tag{20}$$

(The values of *j* from 1 to *i*-1 are omitted because they are redundant as a consequence of the symmetry of $[K^G]$.) Note that the matrix $[C]$ is a tall, rectangular matrix, and thus Eq. (19) can be solved uniquely for $\{P\}$. As a practical matter, $[C]$ is a sparse matrix, and so Eq. (19) is solved using sparse linear algebra subroutines (such as those available in MATLAB (1996)) instead of forming its pseudoinverse.

Application to a Simple Spring System

To illustrate and clarify disassembly of the global stiffness matrix, consider the simple 2 DOF, 3 element spring system shown in Figure 2. The global DOF are defined to be

$$\{u^G\} = \begin{Bmatrix} u_1 \\ u_2 \end{Bmatrix} \tag{21}$$

The necessary quantities for Element 1 are

$$\{u^E\}_1 = u_1 \qquad [T]_1 = [1\ 0] \qquad [K^E]_1 = k_1$$
$$[\kappa]_1 = \frac{1}{\sqrt{2}} \qquad P_1 = 2k_1 \tag{22}$$

and for Element 2 are

$$\{u^E\}_2 = \begin{Bmatrix} u_1 \\ u_2 \end{Bmatrix} \qquad [T]_2 = \begin{bmatrix} 1 & 0 \\ 0 & 1 \end{bmatrix}$$
$$[K^E]_2 = \begin{bmatrix} k_2 & -k_2 \\ -k_2 & k_2 \end{bmatrix} \qquad [\kappa]_2 = \begin{Bmatrix} \frac{1}{\sqrt{2}} \\ -\frac{1}{\sqrt{2}} \end{Bmatrix} \tag{23}$$
$$P_2 = 2k_2$$

and for Element 3 are

$$\{u^E\}_3 = -u_2 \qquad [T]_3 = [0\ -1]$$
$$[K^E]_3 = k_3 \qquad [\kappa]_3 = \frac{1}{\sqrt{2}} \tag{24}$$
$$P_3 = 2k_3$$

The resulting connectivity matrix, formed using Eq. (12), is

$$[A] = \frac{1}{\sqrt{2}} \begin{bmatrix} 1 & 1 & 0 \\ 0 & -1 & -1 \end{bmatrix} \tag{25}$$

and the global stiffness matrix is found using Eq. (11) as

$$
\begin{aligned}
[K^G] &= \frac{1}{\sqrt{2}}\begin{bmatrix}1 & 1 & 0\\ 0 & -1 & -1\end{bmatrix}\begin{bmatrix}2k_1 & 0 & 0\\ 0 & 2k_2 & 0\\ 0 & 0 & 2k_3\end{bmatrix}\frac{1}{\sqrt{2}}\begin{bmatrix}1 & 0\\ 1 & -1\\ 0 & -1\end{bmatrix} \\
&= \frac{1}{2}\begin{bmatrix}1 & 1 & 0\\ 0 & -1 & -1\end{bmatrix}\begin{bmatrix}2k_1 & 0\\ 2k_2 & -2k_2\\ 0 & -2k_3\end{bmatrix} \\
&= \begin{bmatrix}k_1 + k_2 & -k_2\\ -k_2 & k_2 + k_3\end{bmatrix}
\end{aligned}
\tag{26}
$$

which can also easily be formulated using the classical finite element approach. Using the known global stiffness matrix from Eq. (26), it is then straightforward to formulate $\{B\}$ as

$$
\{B\} = \begin{Bmatrix}K_{11}^G\\ K_{12}^G\\ K_{22}^G\end{Bmatrix} = \begin{Bmatrix}k_1 + k_2\\ -k_2\\ k_2 + k_3\end{Bmatrix} \tag{27}
$$

and $[C]$ using Eq. (20) as

$$
[C] = \frac{1}{2}\begin{bmatrix}1 & 1 & 0\\ 0 & -1 & 0\\ 0 & 1 & 1\end{bmatrix} \tag{28}
$$

The values of $\{P\}$ can then be recovered from the elements of $[K^G]$ using Eq. (19) by solving

$$
\frac{1}{2}\begin{bmatrix}1 & 1 & 0\\ 0 & -1 & 0\\ 0 & 1 & 1\end{bmatrix}\begin{Bmatrix}P_1\\ P_2\\ P_3\end{Bmatrix} = \begin{Bmatrix}k_1 + k_2\\ -k_2\\ k_2 + k_3\end{Bmatrix} \tag{29}
$$

Note that the resulting $[C]$ matrix is full rank and invertible; therefore, this problem can be

solved exactly. The resulting solution of Eq. (29) is

$$\begin{Bmatrix} P_1 \\ P_2 \\ P_3 \end{Bmatrix} = \begin{Bmatrix} 2k_1 \\ 2k_2 \\ 2k_3 \end{Bmatrix} \tag{30}$$

and these values of P_i are consistent with those defined at the beginning of the example. Thus, if the global stiffness matrix $[K^G]$ was known from an experiment, then stiffness disassembly could be applied as in Eq. (29) to determine the elemental stiffness parameters P_i and thus the elemental spring stiffness constants k_i.

DISASSEMBLY OF THE GLOBAL FLEXIBILITY MATRIX IN GLOBAL COORDINATES

In most cases the above formulation of the disassembly problem is impractical for application to experimental data, since it requires the numerical inversion of $[G^G]$ to get $[K^G]$, as discussed in the introduction. The following alternative algorithm avoids this problem by formulating the disassembly problem in terms of the flexibility matrix. It has additional advantages over stiffness disassembly that are described at the end of the section. First note that for a given deformation of the structure with values $\{u^G\}$, the total strain energy is

$$U = \frac{1}{2}\{u^G\}^T[K^G]\{u^G\} \tag{31}$$

and the complementary strain energy for the corresponding nodal force vector $\{f^G\}$ is

$$U_c = \frac{1}{2}\{f^G\}^T[G^G]\{f^G\} \tag{32}$$

For a linear structure, the nodal forces and displacements are related as in Eq. (1). Assum-

ing that energy is conserved and that the structure behaves linearly, the strain energy and complimentary strain energy are equal, $U = U_c$. Equating Eq. (31) and Eq. (32) to enforce this assumption yields

$$\{u^G\}^T[K^G]\{u^G\} = \{f^G\}^T[G^G]\{f^G\} \tag{33}$$

Substituting the definition of $\{u^G\}$ from Eq. (1) into Eq. (33) yields

$$\{f^G\}^T[G^G][K^G][G^G]\{f^G\} = \{f^G\}^T[G^G]\{f^G\} \tag{34}$$

Denoting the columns of $[A]$ by $\{A_\beta\}$, Eq. (11) can be written as

$$[K^G] = \sum_{\beta = 1}^{n_p} p_\beta \{A_\beta\}\{A_\beta\}^T \tag{35}$$

This implies via Eq. (34) that

$$\begin{aligned} &\sum_{\beta = 1}^{n_p} p_\beta (\{f^G\}^T[G^G]\{A_\beta\}\{A_\beta\}^T[G^G]\{f^G\}) \\ &\qquad = \{f^G\}^T[G^G]\{f^G\} \end{aligned} \tag{36}$$

Since Eq. (36) must apply for any applied force pattern $\{f^G\}$, a well-posed problem can be formed to solve for $\{P\}$ by choosing n_p different force vectors which span the possible complementary strain energy states of the structure. The columns of $[A]$ satisfy this requirement because they include as a coordinate basis the elemental eigenvectors $[\kappa]$. Applying a force vector $\{f^G\} = \{A_\alpha\}$ to Eq. (36) yields

$$\sum_{\beta = 1}^{n_p} p_\beta (\{A_\alpha\}^T [G^G] \{A_\beta\} \{A_\beta\}^T [G^G] \{A_\alpha\}) = \{A_\alpha\}^T [G^G] \{A_\alpha\} \quad \alpha = 1 \ldots n_p \tag{37}$$

So, as with stiffness disassembly, the problem is of the form

$$[C]\{P\} = [B] \tag{38}$$

where now the (α, β) entry of $[C]$ is

$$C_{\alpha\beta} = \{A_\alpha\}^T [G] \{A_\beta\} \{A_\beta\}^T [G] \{A_\alpha\} \tag{39}$$

and the α^{th} entry in $\{B\}$ is

$$B_\alpha = \{A_\alpha\}^T [G] \{A_\alpha\} \tag{40}$$

This formulation in terms of the flexibility matrix has several advantages over the stiffness disassembly formulation of Eq. (19). First, it avoids the need to form $[K^G]$ by pseudo-inverting the generally rank-deficient $[G^G]$. Second, the matrix $[C]$ can be shown to be positive definite. This means that the stiffness parameters $\{P\}$ are positive provided that the elements of $\{B\}$ are positive. Physically, each row of $\{B\}$ is the complementary strain energy associated with the applied force vector $\{A_\alpha\}$, which must be non-negative by the definition of strain energy. Finally, this set of equations is square and generally invertible, unless the connectivity matrix $[A]$ is improperly formed to allow internal rigid body modes in the structure.

OBTAINING GLOBAL FLEXIBILITY FROM EXPERIMENTALLY MEASURED FLEXIBILITY

The formulation of flexibility disassembly so far is insufficient to solve most practical

problems, because it fails to address the fact that the flexibility matrix is measured at a set of measurement sensor DOF, not at the actual global DOF of the finite element model. A common case in which this occurs is shown in Figure 3. Although the 2 dimensional beam element has 2 DOF at each node, v_i^G and θ_{zi}^G, they are never directly measured. The measurements are only made at the DOF defined as u_i^M and v_i^M. Thus it is necessary to define a transformation from the flexibility matrix $[G^M]$, defined with respect to the measurement degrees of freedom $\{u^M\}$, to the flexibility matrix $[G^G]$, defined with respect to the finite element model global DOF $\{u^G\}$, and suitable for use in the flexibility disassembly equations of the previous section.

To derive the required relationship, first a transformation matrix $[H]$ is introduced that relates the global DOF $\{u^G\}$ to the measured DOF $\{u^M\}$ as

$$\{u^M\} = [H]\{u^G\} \tag{41}$$

The transformation matrix $[H]$ has dimension $(n_m \times n_g)$, and is usually computed by using the kinematic relationships between the measurement DOF and the FEM global DOF, as shown in Greenwood (1988). The inverse transformation to complement Eq. (41) can be written as

$$\{u^G\} = [L]\{u^M\} \tag{42}$$

where

$$[L] = [H]^+ \tag{43}$$

To ensure that a unique pseudoinverse exists in Eq. (43), it is required that $n_m \geq n_g$. It should be noted that this requirement can produce a large experimental channel count, and so in a practical situation the number of global DOF must be restricted to keep the number of required measurements at a reasonable level.

The relationship between $[G^M]$ and $[G^G]$ is derived starting from the definition of the global flexibility matrix using the full set of structural modes:

$$[G^G] = [\Phi^G][\Lambda]^{-1}[\Phi^G]^T \tag{44}$$

Using the transformation in Eq. (42), the global mode shape matrix can be written as

$$[\Phi^G] = [L][\Phi^M] \tag{45}$$

Substituting Eq. (45) into Eq. (44) and simplifying yields the transformation equation from $[G^M]$ to $[G^G]$:

$$[G^G] = [L][G^M][L]^T \tag{46}$$

Thus, once $[G^M]$ is determined from the measured mode shapes, modal frequencies, and residual flexibility using Eq. (4), then $[G^G]$ can be determined using Eq. (46). The computation of $[G^M]$ from the measured modal quantities is further discussed in Doebling, et al. (1996).

Numerical Example of Flexibility Disassembly

In this section, the disassembly of measured flexibility is demonstrated for simulated data from a 2-dimensional, 2-element, 4DOF cantilevered beam, shown in Figure 3. The global and measured DOF are related by the following kinematic relationships (assuming θ is small enough such that $\sin\theta \approx \theta$ and $\cos\theta \approx 1$):

$$\begin{aligned} u_1^M &= -d\theta_{z1}^G \\ u_2^M &= -d\theta_{z2}^G \\ v_1^M &= v_1^G \\ v_2^M &= v_2^G \end{aligned} \tag{47}$$

Define the global and measurement DOF displacement vectors as

$$\{u^G\} = \begin{Bmatrix} v_1^G \\ \theta_{z1}^G \\ v_2^G \\ \theta_{z2}^G \end{Bmatrix} \qquad \{u^M\} = \begin{Bmatrix} u_1^M \\ v_1^M \\ u_2^M \\ v_2^M \end{Bmatrix} \tag{48}$$

Observing Eq. (47) and Eq. (48), along with the definitions in Eq. (41) and Eq. (42) indicates that the $[H]$ and $[L]$ matrices are

$$[H] = \begin{bmatrix} 0 & -d & 0 & 0 \\ 1 & 0 & 0 & 0 \\ 0 & 0 & 0 & -d \\ 0 & 0 & 1 & 0 \end{bmatrix} \qquad [L] = \begin{bmatrix} 0 & 1 & 0 & 0 \\ -\frac{1}{d} & 0 & 0 & 0 \\ 0 & 0 & 0 & 1 \\ 0 & 0 & -\frac{1}{d} & 0 \end{bmatrix} \tag{49}$$

Using the element $[\kappa]$ and $\{p\}$ for a beam from Appendix A, and removing the parameters and corresponding columns of $\{\kappa\}$ that do not include EI_{zz} (since that is the only parameter of interest as this is a two-dimensional, bending-only analysis) yields

$$[\kappa] = \begin{bmatrix} 0 & \frac{\sqrt{2}}{\sqrt{L^2+4}} \\ -\frac{1}{\sqrt{2}} & \frac{L}{\sqrt{2}\sqrt{L^2+4}} \\ 0 & \frac{-\sqrt{2}}{\sqrt{L^2+4}} \\ \frac{1}{\sqrt{2}} & \frac{L}{\sqrt{2}\sqrt{L^2+4}} \end{bmatrix} \{p\} = \begin{Bmatrix} \frac{2EI_{zz}}{L} \\ \frac{6EI_{zz}(L^2+4)}{L^3} \end{Bmatrix} \tag{50}$$

Suppose that the geometric and material properties are

$$\begin{aligned} EI_{zz} &= 607 Nm^2 \\ \rho A &= 1.75 kg/m \\ L &= 0.75 m \\ d &= 0.02 m \end{aligned} \tag{51}$$

Then the expressions of Eq. (50) can be evaluated to get

$$[\kappa] = \begin{bmatrix} 0 & 0.6621 \\ -0.7071 & 0.2483 \\ 0 & -0.6621 \\ 0.7071 & 0.2483 \end{bmatrix} \quad \{p\} = \begin{Bmatrix} 1.62\times10^{3} \\ 3.94\times10^{4} \end{Bmatrix} \tag{52}$$

The transformation $[T]$ for each element is

$$[T_1] = \begin{bmatrix} 0 & 0 & 0 & 0 \\ 0 & 0 & 0 & 0 \\ 1 & 0 & 0 & 0 \\ 0 & 1 & 0 & 0 \end{bmatrix} \qquad [T_2] = \begin{bmatrix} 1 & 0 & 0 & 0 \\ 0 & 1 & 0 & 0 \\ 0 & 0 & 1 & 0 \\ 0 & 0 & 0 & 1 \end{bmatrix} \tag{53}$$

so $[A]$ is formed using Eq. (12) to get

$$[A] = \begin{bmatrix} 0 & -0.6621 & 0 & 0.6621 \\ 0.7071 & 0.2483 & -0.7071 & 0.2483 \\ 0 & 0 & 0 & -0.6621 \\ 0 & 0 & 0.7071 & 0.2483 \end{bmatrix} \tag{54}$$

and the analytical values of P_i are formed using Eq. (13) to get

$$\{P\} = \begin{Bmatrix} 1.62\times10^{3} \\ 3.94\times10^{4} \\ 1.62\times10^{3} \\ 3.94\times10^{4} \end{Bmatrix} \tag{55}$$

Now the measured flexibility matrix will be simulated and disassembled to show that the extracted parameters are the same as in Eq. (55). Using the continuous solution for a Bernoulli-Euler beam (Blevins, 1993), the first modal eigenvalue and mode shape at the measurement DOF are

$$[\Phi^M] = \begin{bmatrix} -1.92\times10^{-2} \\ 4.19\times10^{-1} \\ -2.27\times10^{-2} \\ 1.23 \end{bmatrix} \qquad [\Lambda] = 847.8 \tag{56}$$

The measured flexibility matrix is computed using Eq. (4) (without the effects of residual flexibility) to get

$$[G_n^M] = \begin{bmatrix} 4.35e-7 & -9.49e-6 & 5.14e-7 & -2.79e-5 \\ -9.49e-6 & 2.07e-4 & -1.12e-5 & 6.08e-4 \\ 5.14e-7 & -1.12e-5 & 6.08e-7 & -3.29e-5 \\ -2.79e-5 & 6.08e-4 & -3.29e-5 & 1.78e-3 \end{bmatrix} \tag{57}$$

The residual flexibility matrix (which can be simulated by summing a large number of continuous modes or subtracting the modal flexibility from the analytical stiffness matrix) is then

$$[G_r^M] = \begin{bmatrix} 6.16e-8 & 2.04e-7 & -1.78e-8 & 9.54e-8 \\ 2.04e-7 & 2.43e-5 & 1.94e-6 & -3.15e-5 \\ -1.78e-8 & 1.94e-6 & 3.82e-7 & -4.06e-6 \\ 9.54e-8 & -3.15e-5 & -4.06e-6 & 5.45e-5 \end{bmatrix} \tag{58}$$

Summing the residual and modal flexibility yields the measured flexibility matrix:

$$[G^M] = [G_n^M] + [G_r^M] = \begin{bmatrix} 4.94e-7 & -9.28e-6 & 4.94e-7 & -2.77e-5 \\ -9.28e-6 & 2.31e-4 & -9.26e-6 & 5.80e-4 \\ 4.94e-7 & -9.26e-6 & 9.86e-7 & -3.71e-5 \\ -2.77e-5 & 5.80e-4 & -3.71e-5 & 1.85e-3 \end{bmatrix} \tag{59}$$

The measured flexibility $[G^M]$ is then converted to global DOF coordinates using Eq. (46) to get

$$[G^G] = \begin{bmatrix} 2.31e-4 & 4.64e-4 & 5.76e-4 & 4.64e-4 \\ 4.64e-4 & 1.24e-3 & 1.39e-3 & 1.24e-3 \\ 5.76e-4 & 1.39e-3 & 1.84e-3 & 1.85e-3 \\ 4.64e-4 & 1.24e-3 & 1.85e-3 & 2.48e-3 \end{bmatrix} \tag{60}$$

Substituting Eq. (60) and Eq. (54) into Eq. (38) and solving for $\{P\}$ yields

$$\{P\} = \begin{Bmatrix} 1.62\times10^{3} \\ 3.94\times10^{4} \\ 1.62\times10^{3} \\ 3.94\times10^{4} \end{Bmatrix} \tag{61}$$

Comparing Eq. (61) and Eq. (55) demonstrates that the proper parameters are recovered from the simulated flexibility matrix.

EXPERIMENTAL APPLICATION

A series of modal vibration tests was performed on a simple cantilevered beam structure. The test setup for this structure is shown in the photo of Figure 4. A schematic of the test structure is shown in Figure 5, including the instrumentation and test input location. The test parameters and modal parameter identification procedure used are described by Doebling, et al. (1996). Two disassembly analyses were performed on the data to solve for the cross section stiffness parameter, EI_{zz}: one using a single-element, 2-DOF discretization, and one using a two-element, 4-DOF discretization, as shown in Figure 6.

For the single-element discretization, the experimentally determined, statically complete flexibility matrix for this test, as derived by Doebling and Peterson (1996), is

$$[G^G] = \begin{bmatrix} 0.0016 & 0.0019 \\ 0.0019 & 0.0023 \end{bmatrix} \tag{62}$$

Using the assumed analytical values of the parameters, and assuming that the boundary condition is perfectly cantilevered yields the analytically predicted static flexibility matrix

$$[G^G]_A = \begin{bmatrix} 0.0018 & 0.0018 \\ 0.0018 & 0.0024 \end{bmatrix} \tag{63}$$

For the one-element discretization, the stiffness connectivity matrix $[A]$ can be reduced from Eq. (54) to get

$$[A] = \begin{bmatrix} 0 & -0.6621 \\ 0.7071 & 0.2483 \end{bmatrix} \tag{64}$$

Performing disassembly on $[G^G]$ from Eq. (62) yields a parameter value of $EI = 624 Nm^2$, which is a 2.8% difference from the analytically predicted value, as shown in Table 1. For the two-element discretization, the stiffness connectivity matrix is the same as in Eq. (54). The EI values for the two-element disassembly both have about 10% difference from the analytically predicted value, and are also shown in Table 1. Thus, for both the one-element and two-element discretizations, the cross-sectional stiffness parameter EI determined using disassembly of the measured flexibility matrix has reasonably accurate values.

A final note about this experimental example of flexibility disassembly: It seems counterintuitive at first that the result for the 2-element discretization is less accurate with respect to the analytically predicted value that the single-element discretization, because in finite element analysis it is generally assumed that a more refined mesh will lead to more accurate results, especially when predicting modal dynamic behavior. However, because this is an inverse problem, the elemental properties are being computed from the data, rath-

er than the reverse process in a typical analytical modal analysis. Thus, usual assumptions regarding mesh refinement are not really applicable. Originally, it was hypothesized that this apparent decrease in accuracy arose from the introduction of additional elements into the model and thus the introduction of additional unknowns into the problem. However, because additional measurements are introduced at the same time, the ratio of equations to unknowns in the problem stays constant. However, it is possible that in this particular problem the additional measurements at the midpoint of the beam introduced in the two-element analysis may corrupt the results because of lower signal magnitude and therefore lower signal-to-noise ratio. Of course, it is also possible that the assumed "true" value of elastic modulus for the beam is erroneous, and that the computed value of the modulus from the 2-element discretization is actually closer to the true value.

CONCLUSIONS

A method has been developed which makes it possible to measure local structural stiffness by disassembly of a measured flexibility matrix. The method presumes a connectivity pattern for the structure and solves for the eigenvalues and eigenvectors of the elemental stiffness matrices. It was shown that a unique solution of this problem exists for all structures, except when redundant elements are presumed in the connectivity pattern. The method has also been extended to address the more realistic instance where a mismatch exists between the measured DOF and the nodal DOF of the presumed connectivity pattern. Numerical and experimental applications to a cantilevered beam problem were presented to demonstrate the feasibility of the proposed method.

ACKNOWLEDGMENTS

This paper reports work supported by Sandia National Laboratories under Contract No. AJ-4223 with Dr. George H. James III and Dr. John R. Red-Horse as technical monitors. The authors would like to thank Prof. K.C. Park and Prof. Carlos Felippa for their encouragement and valuable technical insights. Also, the authors wish to recognize University of Colorado undergraduate students Ms. Nikki Robinson and Ms. Trudy Schwartz for their invaluable contributions to the experimental portion of this research. Support for the first author was also provided by Los Alamos National Laboratory Directed Research and Development Project #95002. This work was performed under the auspices of the United States Department of Energy. This document originally appeared as a paper at the 36th AIAA/ASME/ASCE/AHS/ASC Structures, Structural Dynamics and Materials Conference, New Orleans, LA, April 1995.

REFERENCES

Alvin, K. F.,Peterson, L. D., and Park, K. C., 1995, “A Method for Determining Minimum-Order Mass and Stiffness Matrices from Modal Test Data,” *AIAA Journal*, Vol. 33, No. 1, pp. 128-135.

Blevins, R. D., 1993, *Formulas for Natural Frequency and Mode Shape*, Krieger Publishing, Malabar, FL.

Doebling, S.W., 1996, “Minimum-Rank Optimal Update of Elemental Stiffness Parameters for Structural Damage Identification,” *AIAA Journal*, Vol. 34, No. 12, December, pp. 2615 - 2621.

Doebling, S. W., Peterson, L. D., and Alvin, K. F., 1996, “Estimation of Reciprocal Residual Flexibility from Experimental Modal Data,” *AIAA Journal*, Vol. 34, No. 8, August, pp. 1678 - 1685.

Greenwood, D. T., 1988, *Principles of Dynamics*, 2nd ed., Prentice-Hall, Englewood Cliffs, NJ, Chapter 2.

Kaouk, M. and Zimmerman, D. C., 1994, "Structural Damage Assessment Using a Generalized Minimum Rank Perturbation Theory," *AIAA Journal*, Vol. 32, No. 4, pp 836-842.

Lim, T. W. and Kashangaki, T. A., 1994, "Structural Damage Detection of Space Truss Structures Using Best Achievable Eigenvectors," *AIAA Journal*, Vol. 32, No. 5, pp 1049-1057.

MATLAB, 1996, *Using Matlab*, The Mathworks, Inc., Natick, MA.

Peterson, L. D., Alvin, K. F., Doebling, S. W., and Park, K. C., 1993, "Damage Detection Using Experimentally Measured Mass and Stiffness Matrices" AIAA-93-1482 *Proc. of the 34th AIAA Structures, Structural Dynamics, and Materials Conference*.

Peterson, L. D., 1995, "Efficient Computation of the Eigensystem Realization Algorithm," *Journal of Guidance, Control, and Dynamics*, Vol. 18, No. 3, pp. 395-403.

Peterson, L. D. and Alvin, K. F., 1997, "Time and Frequency Domain Procedure for Identification of Structural Dynamic Models," *Journal Of Sound And Vibration*, Vol. 201, No. 1, pp. 137-144.

Sheinman, I., 1994, "Damage Detection in Framed Structures" *AIAA Journal*, Vol. 32, No. 5, pp 1103-1105.

Strang, G., 1988, *Linear Algebra and its Applications*, Harcourt Brace Jovanovich, San Diego, CA.

Zienkiewicz, O.C. and Taylor, R.L., 1994, *The Finite Element Method, Volume I*, 4th Ed., McGraw-Hill, London, Chapter 6.

Table 1. Difference Between Analytically Predicted EI and Experimentally Determined EI for Cantilevered Beam

Discretization	Element	EI Difference
1-Element	Element 1	2.8%
2-Element	Element 1	10.5%
	Element 2	9.9%

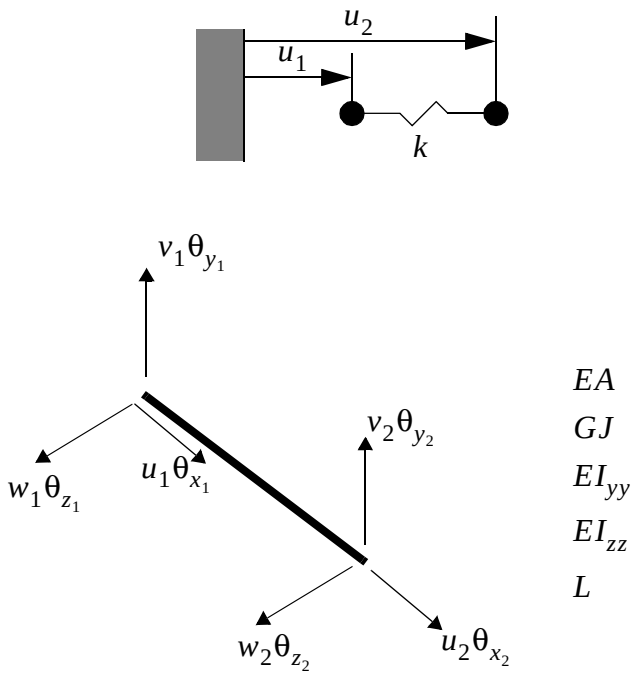

Figure 1: 2-DOF Spring (Truss) and 12-DOF Beam Elements

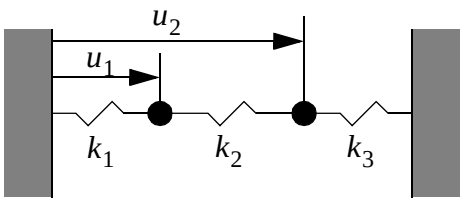

Figure 2: 2-DOF Spring (Truss) System

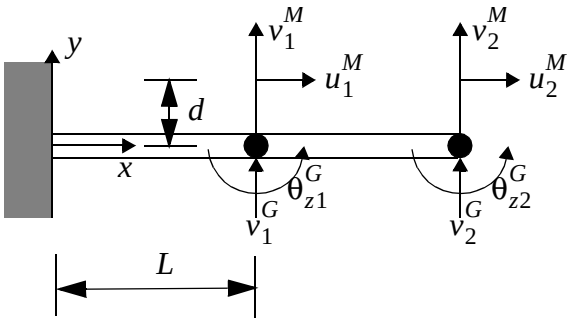

Figure 3: 2 Element Cantilevered Beam to Illustrate the Effect of Sensor Offsets

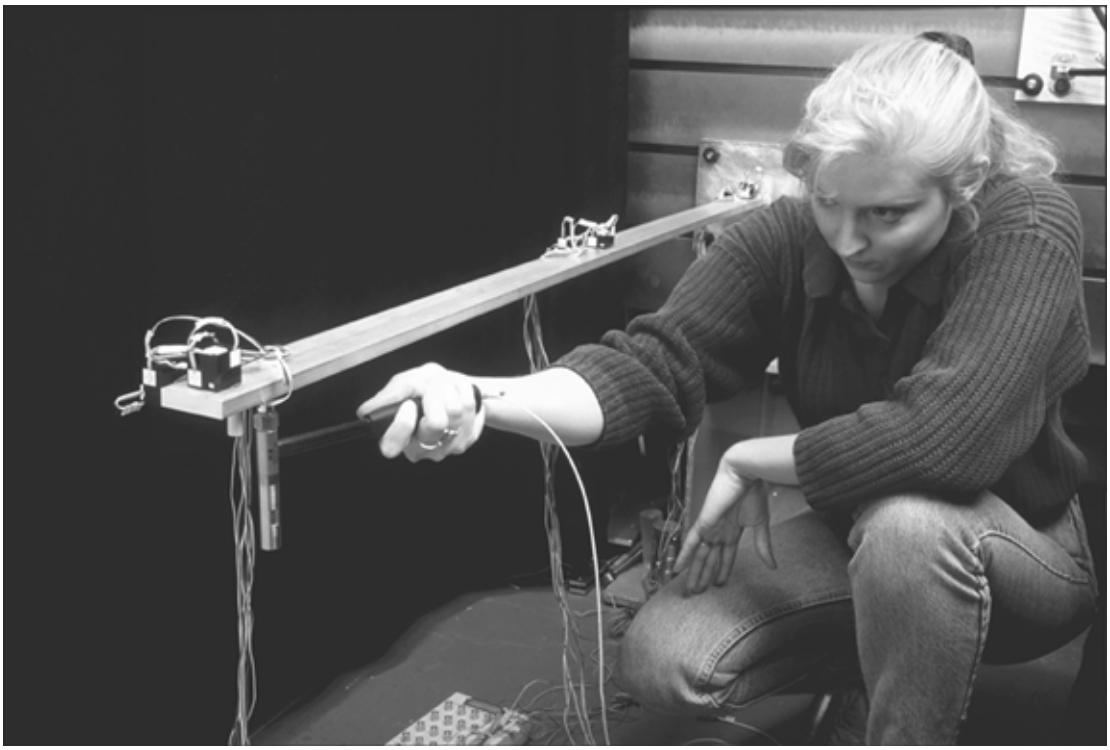

Figure 4: Cantilevered Beam Test Setup

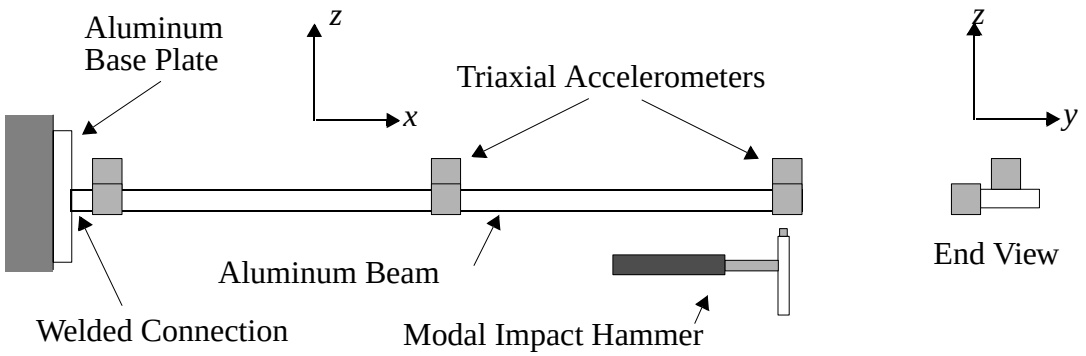

Figure 5: Schematic of Cantilevered Beam Test Structure

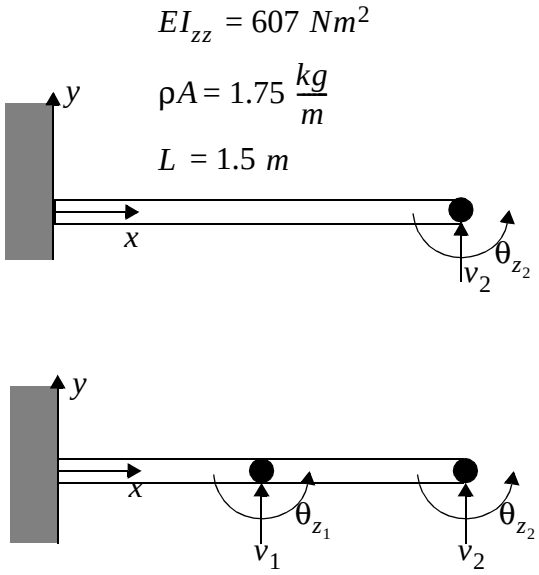

Figure 6: One-Element and Two-Element Cantilevered Beam Discretization Models

APPENDIX A: ELEMENTAL EIGENSOLUTION FOR BEAM ELEMENT

The parameters $[\kappa]$ and $\{p\}$ for the 4-th order Bernoulli-Euler beam element in three dimensional space are

$$[\kappa] = \begin{bmatrix} \frac{1}{\sqrt{2}} & 0 & 0 & 0 & 0 & 0 \\ 0 & 0 & 0 & \frac{\sqrt{2}}{\sqrt{L^2+4}} & 0 & 0 \\ 0 & 0 & 0 & 0 & 0 & \frac{\sqrt{2}}{\sqrt{L^2+4}} \\ 0 & \frac{1}{\sqrt{2}} & 0 & 0 & 0 & 0 \\ 0 & 0 & 0 & 0 & \frac{1}{\sqrt{2}} & -\frac{L}{\sqrt{2}\sqrt{L^2+4}} \\ 0 & 0 & -\frac{1}{\sqrt{2}} & \frac{L}{\sqrt{2}\sqrt{L^2+4}} & 0 & 0 \\ -\frac{1}{\sqrt{2}} & 0 & 0 & 0 & 0 & 0 \\ 0 & 0 & 0 & -\frac{\sqrt{2}}{\sqrt{L^2+4}} & 0 & 0 \\ 0 & 0 & 0 & 0 & 0 & -\frac{\sqrt{2}}{\sqrt{L^2+4}} \\ 0 & -\frac{1}{\sqrt{2}} & 0 & 0 & 0 & 0 \\ 0 & 0 & 0 & 0 & -\frac{1}{\sqrt{2}} & -\frac{L}{\sqrt{2}\sqrt{L^2+4}} \\ 0 & 0 & \frac{1}{\sqrt{2}} & \frac{L}{\sqrt{2}\sqrt{L^2+4}} & 0 & 0 \end{bmatrix} \qquad \{p\} = \begin{bmatrix} \frac{2EA}{L} \\ \frac{2GJ}{L} \\ \frac{2EI_{zz}}{L} \\ \frac{6EI_{zz}(L^2+4)}{L^3} \\ \frac{2EI_{yy}}{L} \\ \frac{6EI_{yy}(L^2+4)}{L^3} \end{bmatrix}$$